IEEE Access
Multidisciplinary | Rapid Review | Open Access Journal

Date of publication xxxx 00, 0000, date of current version xxxx 00, 0000.

Digital Object Identifier 10.1109/ACCESS.2017.Doi Number

Co-optimization of Supply and Demand Resources for Load Restoration of Distribution System under Extreme Weather

Xi Zhu[1], Bo Zeng[1], Yonggang Li[2], and Jiaomin Liu[1]

1 State Key Laboratory of Alternate Electrical Power System with Renewable Energy Sources, North China Electric Power University, Beijing 102206, China

2 State Key Laboratory of Alternate Electrical Power System with Renewable Energy Sources, North China Electric Power University, Baoding 071003, China

Corresponding author: Yonggang Li (e-mail: lygzxm0@163.com).

This work was supported in part by the National Natural Science Foundation of China (51507061), and the Fundamental Research Funds for the Central Universities (2018QN080).

ABSTRACT To deal with the issue of the distribution system (DS) resilience enhancement under extreme weather events, this paper presents a new methodological framework for enhancing the load restoration of DS during a hurricane. As distinct from existing studies, this approach integrates mobile emergency generators (MEGs) and prosumer communities (PCs) incorporating combined heat and power (CHP) units, electric boilers (EBs), photovoltaic (PV) sources, and demand response (DR) resources and comprehensively explores the coordination and flexibility of supply-side and demand-side resources to boost the post-disaster DS recovery. The discussed problem is formulated by using a two-stage robust optimization model. In the first stage, the MEGs are pre-positioned prior to the hurricane with the objective of minimizing the outage cost of the load to promote the capability of DS to resist extreme disturbance. The second stage determines the real-time allocation of MEGs, output power of CHP units and EBs, and the power consumption of electric loads after the hurricane to maximize DS's load recovery considering the worst-case of the uncertainty realization. Since the fragility analysis of network elements has an essential impact on the efficacy of the optimal strategy, we introduce the Z-number-based approach to scientifically determine the failure probability of components considering the effect of the aging of components and the credibility of the failure information obtained from the fragility. The effectiveness of the proposed methodology is examined based on an IEEE 123-bus distribution test system, and the obtained results confirm the validity of the proposed approach in actual implementations.

INDEX TERMS Extreme weather events, resilience, demand response, two-stage robust optimization, Z-number.

NOMENCLATURE

A. INDICES

i, j	Index of nodes in the distribution network
a	Index of loads in prosumer communities
k	Index of energy coupling equipment in prosumer communities
m	Index of MEGs
t	Index of time

B. SETS

Ω_N	Set for nodes in the distribution network
Ω_{pro}	Set for prosumer communities
Ω_{Nm}	Set of nodes that MEG m can be connected to
Ω_{sub}	Set for substations in DS
Ω_{fl}	Set for fixed loads
Ω_{nisl}	Set for non-interruptible shiftable loads
Ω_{isl}	Set for interruptible shiftable loads
Ω_{HL}	Set for heat loads
Ω_{CHP}	Set for CHP units
Ω_{EB}	Set for electric boilers
M	Set/index for MEGs
T	Time set/index
Φ^f	Set for first-stage decision variables: $\{\alpha_{m,i}, f^{ic}_{org,ij}, \beta^{pri}_{ij}, f^{source}_{org,i}\}$

Φ^s	Set for second-stage decision variables: $\{\delta^t_{m,i}, p^t_{m,out}, p^t_i, L^{CHP,e,t}_{out,k,i}, M^{EB}_{in,k,i}, P^t_{nisl,a}, P^t_{isl,a}\}$

C. CONSTANTS

$\lambda_{shedding,i}$	Outage cost per capacity of load
s^{max}_{ij}	Maximum apparent power of line (i,j)
V^{min}_i/V^{max}_i	Minimum/maximum voltage value of node i
r_{ij}/x_{ij}	Resistance/reactance of line (i,j)
P^{max}_m/Q^{max}_m	Maximum active/reactive power output of MEG
$L^{CHP}_{out,k,max}/L^{CHP}_{out,k,min}$	Maximum/Minimum output power of the CHP unit
$L^{EB}_{out,k,max}/L^{EB}_{out,k,min}$	Maximum/Minimum output power of the EB
$P^{h,t}_{Load,a,i}$	Thermal power consumed by the heat load

D. VARIABLES

$P^t_{shedding,i}$	Shedding loads due to the hurricane
$\alpha_{m,i}$	Binary, 1 if MEG m is pre-positioned to node i, 0 otherwise
β^{pri}_{ij}	Binary, 1 if branch (i,j) is closed prior to the extreme disaster, 0 otherwise
$f^{fic}_{org,ij}/f^{fic}_{post,ij}$	Fictitious flow on line (i,j) prior to/after the extreme disaster
$f^{source}_{org,i}/f^{source}_{post,i}$	Amount of fictitious flow out of a substation node i prior to/after the extreme disaster
$f^{load}_{org,i}/f^{load}_{post,i}$	Amount of fictitious flow into a load node i prior to/after the extreme disaster
$p^t_{org,ij}/q^t_{org,ij}$	Active/reactive power transmitted on the branch (i,j) before the hurricane
$p^t_{org,i}/q^t_{org,i}$	Active and reactive power demand of node i before the hurricane
$P^t_{org,i}/Q^t_{org,i}$	Active and reactive power injected into node i before the hurricane
$\delta_{m,i}$	Binary, 1 if MEG m is connected to node i, 0 otherwise
β^{post}_{ij}	Binary, 1 if branch (i,j) is closed after the extreme disaster, 0 otherwise
$p^t_{m,out}/q^t_{m,out}$	Active/reactive power output of MEG
p^t_{ij}/q^t_{ij}	Active/reactive power transmitted on the branch (i,j) after the hurricane
p^t_i/q^t_i	Active/reactive power demand of node i after natural disasters
P^t_i/Q^t_i	Active/reactive power injected into node i after the hurricane
$L^{CHP,e}_{out,k}/L^{CHP,h}_{out,k}$	Electrical/thermal output power of the CHP unit
$L^{EB,h}_{out,k}$	Thermal output of the EB
$M^{CHP}_{in,k}/M^{EB,e}_{in,k}$	Input power of the CHP unit/EB
$P^t_{nisl,a}$	Power consumption of the non-interruptible shiftable load
$P^t_{isl,a}$	Power consumption of the interruptible shiftable load

I. INTRODUCTION

More frequent extreme weather events seriously threaten the security of the exposed power system's infrastructure, especially the distribution system (DS). Moreover, with the rapid development of innovative technology in the modernization of power system, not only increasing types of distributed energy supply resources (e.g., renewable energy resources, multi-energy coupling devices, and mobile power sources) appear, but also demand-side resources attract more attention as flexible adjustment resources for the power system operation in emergency conditions [1]. The interaction and coordination of the supply-side and demand-side resources bring more flexibility and uncertainties for the resilient operation of the power grid. Consequently, appropriate strategies need to be made to enhance the load restoration of the power systems during natural disasters based on comprehensive utilization of multi-energy supply and demand resources.

At present, extensive research efforts have been dedicated to the enhancement of DS resilience under natural disasters. Many strategies have been put forward to help the power systems resist the disturbance caused by extreme weather events in terms of physical hardiness, such as network and component reinforcement and repair [2-5]. Besides, with the development of renewable energy and integrated energy system, a large number of distributed energy resources have emerged in the system, including photovoltaic (PV) sources, energy coupling equipment, mobile power sources, and so on. In this case, some experts propose to utilize these flexible distributed resources to help DS resist extreme disasters from the perspective of operation capability improvement [6-17]. For example, Reference [6] adopted microgrids with distributed generators to recover the important loads after natural disasters considering the uncertainties of wind power, solar power, and load demand. And the distributed energy, including battery storage and photovoltaic (PV) generation, was sized and sited optimally in [8] to boost the grid resilience under extreme disasters based on the multi-objective optimization method. Reference [10] proposed a DS load restoration approach by using multiple distributed energy resources, including renewable generation, micro-turbine, and energy storage, considering the DS recovery process sequence. Reference [11] employed distributed energy resources to improve the important loads restoration considering the system infrastructure. To further increase the DS's capability to withstand severe events, reference [4,7] combined the physical and operational measures via strengthening the distribution lines and allocating the distributed power sources. Besides a single power system, the coupling of power and transportation networks was considered by the authors of [13] to develop resilient recovery schemes, which make full use of repair crews, mobile power sources, and topology reconstruction technology of DS. However, these studies [6-17] mainly focus on the supply-side resources to enhance the power grid's capacity against disasters. Both the application of

This article has been accepted for publication in a future issue of this journal, but has not been fully edited. Content may change prior to final publication. Citation information: DOI 10.1109/ACCESS.2021.3102497, IEEE Access

distributed power supply resources and network upgrade need substantial investment cost, and the power recovery capability improved by these two measures is limited. To further improve load restoration within limited costs, demand response (DR) is used to relieve power supply pressure during severe contingency conditions. For example, reference [18] studied the incentive-based DR program to maximize DS's load loss in case of the generation units' failure based on the security-constrained unit commitment model. A multi-state model for demand reduction was built in [19] to deal with insufficient power supply. Compared with [19], reference [20] adopted load demand modification instead of load shedding to prevent DS from violating the operational limit.

In addition, when DS goes through extreme weather events, partial electrical components of the power network may be broken. In the above literature [3, 7 12-14], the defective components in the distribution network caused by extreme events are determined by artificially given. However, a component malfunction is not random but depends on the location, intensity, type of disaster, and position of components in the DS. To deal with this, the impact of the extreme disasters on electrical components was quantified via Monte Carlo simulations in [8] with considering disaster strength, physical features of the equipment, and equipment reliability. To more clearly construct the vulnerability model of power elements in danger of extreme weather, reference [21] adopted a linear piecewise function to approximate the relationship between the failure probability of transmission components and the intensity of windstorms. Based on [21], reference [2, 4, 22] calculated the failure probability of support poles and overhead power lines via fragility curves expressed by the lognormal distribution.

According to the above research work, it can be deduced that DS mainly uses supply-side resources to improve the load restoration during extreme events. Still, resources in the DS are not fully utilized, such as flexible demand-side resources. Specifically, DR resources are adopted in the above studies to solve the problem of tight power supply mainly from the perspective of reliability. The reliability theory primarily considers the general faults with a high probability of occurrence during the operation of the power grid based on average calculation. However, grid resilience concentrates on the extreme events with a low probability of occurrence. In this case, it is not scientific to calculate grid resilience through average. Moreover, when a natural disaster strikes the power grid, power outages for some users, even all users, may occur in the DS owing to the destruction of part of the infrastructure. In this situation, using only energy supply resources to restore the load is limited due to the inadequate number of devices and finite equipment investment costs of DS. Besides, if the power infrastructure is broken and there is no power supply during the contingency events, the end-users cannot participate in the DR program. If there is a certain amount of electricity but not enough during the external disturbance, the DR program can relieve the power supply pressure by shifting the load during the peak electricity consumption period to the low electricity consumption period. It can be inferred that DR resources can help the limited supply-side resources recover more energy demand, and supply-side resources provide energy to support the implementation of the DR program. As a result, only when the supply-side and DR resources are applied in a coordinated manner can the DS's energy supply capacity be fully enhanced during extreme disasters.

In the research of grid resilience promotion strategy, the impact of natural disasters on the power systems is usually quantified via the failure probability of electrical components, such as the conductor wires and poles of transmission corridors. And the failure probability of electrical components is caculated based on the structural reliability analysis. In other words, the fragility curve is adopted to describe the relationship between components failiure probability and disaster intensity. The faulty components of DS during the extreme events are determined by given artificially or one single fragility curve in the above studies [2-4, 7, 12-14]. However, on the one hand, in practice, the damage extent of power infrastructure due to weather-related events is greatly influenced by the aging of electrical components. And the vulnerability of the same component of different ages is characterized by different fragility curves. On the other hand, the fragility curve is obtained empirically based on the historical observation failure data. Since certain weather-related failure records of components (e.g., conductor wires and poles) are not always sufficient, the failure probability calculated by fragility curves may deviate from the actual situation. Hence, one single fragility curve cannot fully express the damage of power elements exposed to extreme weather.

To solve the above problem, this paper presents a comprehensive resources allocation framework for enhancing the load restoration (ELR) of DS during extreme weather disaster. We take into consideration both supply-side resources with multiple types of energy and demand-side resources and explore the coordination and flexibility of supply-side and demand-side resources to boost the post-disaster DS recovery, wherein the supply-side resources comprises mobile emergency generators (MEGs), energy coupling units, and renewable energy sources. In particular, three prosumer communities (PCs) are respectively connected to three load nodes of DS, which consists of combined heat and power (CHP) units, electric boilers (EBs), PV sources, thermal load, and electric load participating in the DR program. Based on this, the ELR problem is formulated using a two-stage robust optimization (RO) model. In the first stage, the MEGs are pre-positioned prior to extreme weather events with the objective of minimizing the outage cost of load in order to promo te the capability of DS to resist severe disturbance. The second stage determines

This article has been accepted for publication in a future issue of this journal, but has not been fully edited. Content may change prior to final publication. Citation information: DOI 10.1109/ACCESS.2021.3102497, IEEE Access

the real-time allocation of MEGs, output power of CHP units and EBs, and the power consumption of electric loads after the extreme weather events to maximize DS's load recovery considering the worst-case realization of the uncertainty of the components' functional states. To properly determine the failure probability of power network elements (e.g., conductor wires and poles), we introduce the Z-number-based vulnerability modeling approach considering the effect of the aging of components and the credibility of the failure information obtained from the fragility. A column-and-constraint generation (C&CG) algorithm is applied to solve the developed two-stage RO model.

Specifically, this paper makes the following contributions:

1) We fully explore the interaction and coordination of the MEGs, CHP units, EBs, PV sources and DR resources to develop the optimal recovery improvement strategy for the DS. And according to allocation process of the MEGs before and after the hurricane disaster, a two-stage RO model with the objective of minimizing load loss cost is established, while considering the uncertainty of power network fragility caused by the extreme weather event.

2) The Z-number-based vulnerability modeling technique is proposed to determine the failure probability of electrical components of the power network, such as conductor wires and poles, in this paper. Compared with one single fragility curve-based method, the proposed Z-number-based method provides a more appropriate estimation for the functional states of components, which considers the aging of components and the credibility of information obtained from fragility curves.

3) Various simulations are conducted to prove the efficacy of the Z-number-based vulnerability modeling approach and the effect of comprehensive utilization of supply-side and demand-side resources on ELR.

The rest of the paper is organized as follows. Section II details the proposed problem of resource allocation for DS ELR. Then section III introduces the models for quantifying the impact of the extreme weather event on the power network, including the extreme weather model and the vulnerability model of transmission corridors. Section IV elaborates on the mathematical formulation of the proposed problem and solution approach. Based on the proposed formulation, numerical studies are carried out in section V. Finally, Section VI gives the conclusion of the research.

II. PROBLEM DESCRIPTION

In this study, a DS architecture consisting of a distribution network, MEGs, PCs, and traditional electric loads is constructed. Wherein a PC composed of multiple energy prosumers is connected to the main grid via a load node of the DS. Specifically, the PC with energy generation, conversion, consumption, and the user energy management system (UEMS) incorporates CHP units, EBs, PV generation, thermal load, and electric load.

In this configuration, normally, the distribution network supplies sufficient power to load consumers, whereas the distribution line disconnection accidents may happen when extreme weather events occur. This would weaken the DS's power supply ability and lead to the energy shortage of the load users.

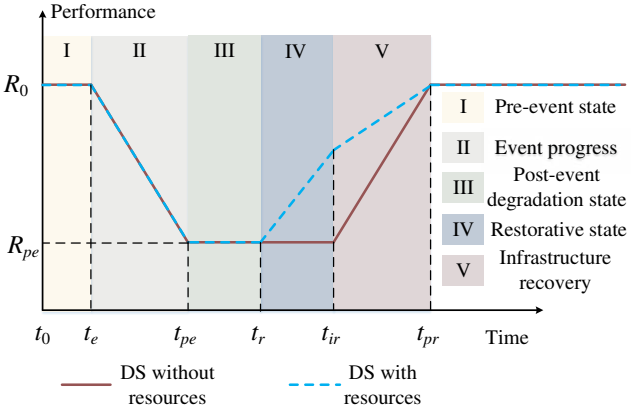

FIGURE 1. Simplified resilience curve during extreme disasters.

During extreme disasters, the DS performance can usually be described via a simplified resilience curve, illustrated in Fig.1. It is generally considered that the DS undergoes the following states:

Phase I: Pre-event state: anticipation and preparation for disasters;

Phase II: Event progress: system resists the natural disaster, and the system performance declines.

Phase III: Post-event degradation state: system performance reaches a minimum level, and damage assessment is conducted to prepare for the restoration.

Phase IV: Restorative state: partial system performance starts to restore.

Phase V: Infrastructure recovery: system infrastructure starts to be repaired, and the system returns to the pre-disaster state.

This paper focuses on the recovery of DS operational performance. In other words, reduction of DS performance loss in Restorative state (Phase IV) is the main goal of this work, and the infrastructure recovery is beyond the scope of this article. Besides, the time for Post-event degradation state is calculated via the random numbers generation method [23] based on the historical experience information.

In response to the extreme disasters, the MEGs could be immediately allocated as flexible resources in DS to pick up partial loads in time and maintain the power supply for several days or even longer. Besides, in the PC, the EBs would reduce the power consumption and thus the heat production. To meet the requirements of heat users, the CHP units in the PC consume more natural gas to generate thermal energy. Meanwhile, more electricity could be produced to relieve the power supply pressure of the DS. Moreover, the DR program is implemented in PC according to end users' load characteristics, and the prosumer makes its own optimal load consumption strategy through UEMS. Then each prosumer sends the relevant information to the corresponding PC. Based

This article has been accepted for publication in a future issue of this journal, but has not been fully edited. Content may change prior to final publication. Citation information: DOI 10.1109/ACCESS.2021.3102497, IEEE Access

on this information, the PC could regulate the energy consumption behavior of all prosumers to maximize the utilization of PV power. Thus distributed energy resources and DR programs could help relieve the power supply pressure during the disturbance and improve the DS resilience during Phase IV. The blue dotted line shows this effect in Fig.1.

This paper proposes a framework for efficient allocation and utilization of the supply-side resources incorporating MEGs, CHP units, EBs, and PV sources, as well as demand-side resources to improve the DS operational resilience during the hurricane disaster, which follows a two-stage routine as below, illustrated in Fig.2.

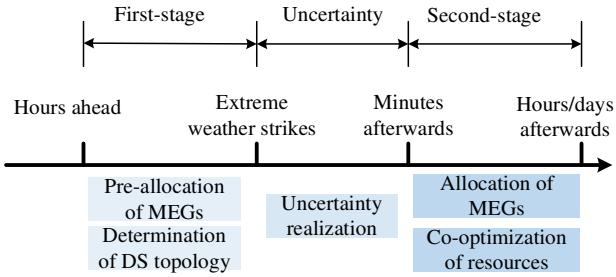

FIGURE 2. Schematic of the two-stage problem.

In the first stage, prior to the extreme weather disaster, the MEGs are pre-positioned to the candidate waiting nodes in the DS to achieve the quickest response to post-disaster conditions. According to the topological characteristics as well as the distribution of sources and loads of the DS, we determine the pre-allocation of MEGs and network topology of the DS to minimize the outage cost of loads. The first-stage decisions are made before realizing relevant uncertainties that are the components' functional states in our problem.

In the second stage, after the extreme weather disaster strikes, the weather information and the impact of weather on the distribution network are known. Based on this, the MEGs are dispatched to candidate nodes from the waiting nodes of the first stage, and the sub-network is also formed. Then the operational strategy of energy coupling equipment and DR in PCs can be determined. For this stage, the real-time allocation of MEGs, output power of CHP units and EBs, and the power consumption of electric loads are co-optimized to maximize DS's load recovery, subject to the worst-case realization of the uncertainty of the functional states of the components.

In this study, to avoid excessive complicities, we make the following assumptions. 1) We assume that the transportation of MEGs could be carried out normally before and after the natural disaster, and the transportation network is not considered. 2) To describe the change of controllable load on the time axis more intuitively, we also assume that the load nodes' power supply is restored simultaneously. 3) We assume that each faulty/damaged line can be isolated via switches, and the healthy but de-energized part of the feeder can then be restored by using available feeders or MEGs. And suppose that the time required for fault isolation is included in the time for damage assessment (Phase III).

III. IMPACT OF EXTREME WEATHER ON POWER NETWORK

This section constructs the hurricane model and vulnerability model of the transmission lines to analyze the influence of the hurricane on the power network.

A. EXTREME WEATHER MODEL

The extent of the damage caused by natural disasters to the power system depends on many factors, such as the type of natural disasters (typhoon, earthquake, ice, and snow [22]), the intensity of natural disasters, and the structure of the distribution network. Therefore, the model of the extreme weather event needs to be determined first. At present, there are mainly two methods for modeling natural disasters. One is to use relevant historical statistic data [24], and another is based on the physical mechanism of natural disasters [25]. In this paper, we take a hurricane as an example and establish the hurricane disaster model based on its physical mechanism. The hurricane's eye location and radius determine the location and area of the network affected by the hurricane. The wind speed of a hurricane determines the extent of damage to critical power network components, such as power poles. When a hurricane disaster occurs, distribution lines in the area with high wind speed may have a greater probability of pole collapse and other fault events. Thus, the wind speed model of the hurricane is the foundation of the damage model of distribution lines under the influence of hurricane disaster.

Based on the pressure, maximum wind speed, maximum wind speed radius, periodic wind speed of a hurricane, the wind speed model of the hurricane could be presented as follows [25]:

$$v = v_m \left\{ \left(\frac{R_{v_m}}{d_v} \right)^{b_v} e^{\left[1 - \left(\frac{R_{v_m}}{l} \right)^{b_v} \right]} \right\}^{a_v} \tag{1}$$

where v_m is the maximum wind speed of a hurricane; R_{v_m} is the maximum wind speed radius of a hurricane; d_v is the distance between the location of the required wind speed and the center of the hurricane; b_v is a proportional parameter, which can be estimated by the central pressure of the hurricane [25]; a_v is a proportional parameter, which is related to the shape of the cyclone, and is usually taken as 0.5 [25].

B. TRANSMISSION CORRIDORS VULNERABILITY MODEL

The influence of a hurricane on the power network can be expressed by the vulnerability model of power transmission corridors mainly composed of conductor wires and poles. And in most existing literature, the failure probability of components subjected to disaster intensity (e.g., wind speed) is usually calculated by using fragility curves. According to the structural reliability analysis theory, a fragility curve obtained based on historical data describes the functional relationship between failure probability of a component (e.g.,

This article has been accepted for publication in a future issue of this journal, but has not been fully edited. Content may change prior to final publication. Citation information: DOI 10.1109/ACCESS.2021.3102497, IEEE Access

support poles and conductor wires) and disaster intensity under given design strength or aging conditions of the power element. However, since the lower frequency of extreme weather events and various types of components results in fewer failure records of the specific components, it is challenging to produce fragility curves of the components that fully conform to the actual situation under certain extreme weather due to the insufficient historical data. Moreover, in practice, the transmission/distribution network contains many power equipment and components, and the same type of element may have various design parameters. Due to the influence of their design, external environment, or other objective factors, the aging degree of these electric elements is different even within the same transmission or distribution network. However, most existing literature uses one single fragility curve to imitate the failure of all support poles or conductor wires in the distribution network, which could not fully reflect the aging condition and actual failure situation of power components.

To solve the above issue, this paper introduces a Z-number-based method to estimate the failure probability of the distribution lines exposed to the hurricane disaster. Z-number is a new concept of fuzzy theory, proposed by Zadeh [26], to deal with the issue of uncertainty and reliability of information during the decision-making process. The Z-number method has advantages for handling uncertainty modelling with incomplete information [27]. Compared with the fragility curve, the proposed Z-number-based approach can consider the credibility of failure information obtained from the fragility curve besides the failure information. The vulnerability model constructed via the proposed method not only contains statistical information based on historical data but also reflects the certainty (sureness, confidence, probability, etc.) of the acquired information. This effectively addresses the problems caused by insufficient information. Besides, the proposed Z-number-based technique could integrate multiple fragility curves to fully consider the aging condition of all components of each type in a distribution network. Thus, the Z-number-based method can provide a more comprehensive and credible estimation for the failure probability of key electric elements exposed to the natural disaster.

The Z-number method adopts an ordered pair of fuzzy numbers (A, B) to construct the uncertain model of variables. And in the ordered pair of fuzzy numbers (A, B), A is the possibility distribution of the uncertain variable. The second component, B, expresses the certainty of the possibility distribution.

In this paper, the failure probability of the key electric elements (p) is assumed as the Z-number variable. The uncertainty of p could be described via the ordered pair of fuzzy numbers (A, B), where A is a fuzzy restriction on the values that uncertain variable p could take, and B is the measure of the certainty of the restriction of A on uncertain variable p. According to the definition of the fuzzy set, A and B could be expressed as follows:

$$A = \left\{ \left\langle p, \mu_A(p) \right\rangle \middle| \, p \in [0,1] \right\} \tag{2}$$

$$B = \left\{ \left\langle p, \mu_B(p) \right\rangle \middle| \, p \in [0,1] \right\} \tag{3}$$

where μ_A and μ_B are the membership functions of A and B, describing the degree of belongingness of p and the reliability level of A, respectively. In this paper, we respectively adopt the trapezoid and triangular fuzzy number to represent A and B, shown as follows:

$$A = (a_1, a_2, a_3, a_4) \tag{4}$$

$$B = (b_1, b_2, b_3) \tag{5}$$

where a_1-a_4 and b_1-b_3 are the parameters of the fuzzy domain of the uncertainty variable. The values of a_1-a_4 are the components' failure probability under given wind speed, determined via multiple fragility curves of the electric component with the different aging conditions. In this way, the same type of power elements with different aging degrees in the distribution network could be taken into account. And the values of b_1-b_3 could be obtained based on the reliability level of the possibility distribution.

Based on the above trapezoid and triangular fuzzy numbers, a Z-number is usually transformed to a classical fuzzy number to obtain the value of the Z-number variable p according to the Fuzzy Expectation theory, the procedures of which are presented as follows.

Step 1) Convert the reliability part of Z-number (B) into a weight coefficient (ϖ) via

$$\varpi = \frac{\int p \mu_B(p) dp}{\int \mu_B(p) dp} \tag{6}$$

Step 2) Obtain the weighted Z-number by adding the above weight coefficient to A,

$$Z^{\varpi} = \left\{ \left\langle p, \mu_{A^{\varpi}}(p) \right\rangle \middle| \mu_{A^{\varpi}}(p) = \varpi \mu_A(p), p \in [0,1] \right\} \tag{7}$$

Step 3) Transform the weighted Z-number into a regular fuzzy number, denoted as:

$$Z' = \left\{ \left\langle p, \mu_{Z'}(p) \right\rangle \middle| \mu_{Z'}(p) = \mu_A\left(\frac{p}{\sqrt{\varpi}} \right), p \in [0,1] \right\} \tag{8}$$

Step 4) Obtain the value of components' failure probability under specific wind speed by the center of gravity technique [28], which could transform the fuzzy model into numerical values as follows:

$$p_Z = p_{Z'} = \frac{\int p \mu_{Z'}(p) dp}{\int \mu_{Z'}(p) dp} \tag{9}$$

Generally speaking, the transmission corridors are composed of poles, conductor wires, and other types of equipment. The damage of a single pole or conductor wire could cause the entire transmission corridor to fail. Therefore, the vulnerability model of a transmission corridor could be derived by the failure probabilities of poles ($p_{pole,9}$) and

This article has been accepted for publication in a future issue of this journal, but has not been fully edited. Content may change prior to final publication. Citation information: DOI 10.1109/ACCESS.2021.3102497, IEEE Access

conductor wires ($p_{con,\vartheta}$) based on the principle of series connection:

$$p_{line,ij}(v)=1-\prod_{\vartheta_1=1}^{n_{pole}}\left(1-p_{pole,\vartheta_1}(v)\right)\prod_{\vartheta_2=1}^{n_{con}}\left(1-p_{con,\vartheta_2}(v)\right) \quad (10)$$

where n_{pole} and n_{con} are the number of poles and conductor wires included in the line (i, j) respectively; $p_{pole,\vartheta}$ and $p_{con,\vartheta}$ could be obtained via (2)-(9).

IV. MATHEMATICAL FORMULATION OF THE OPTIMIZATION MODEL

The concerned two-stage problem could be mathematically formulated as a Min-Max-Min optimization model, shown in (11)-(60). And the objective of the concerned ELR problem is to minimize the costs of load shedding of the DS before and after the hurricane disaster, considering the uncertainty of components' functional states.

$$\min_{\substack{\alpha_{m,i},f^{fic}_{org,ij},\\ \beta^{pri}_{ij},f^{source}_{org,i}}}\ \max_{\mu_{ij}}\ \min_{\substack{\delta_{m,i},P^{t}_{m,out},P^{t}_{i},L^{CHP,e,t}_{out,k,i},\\ M^{EB}_{in,k,i},P^{t}_{nist,a,i},P^{t}_{ist,a,i}}}\left\{\sum_{i}^{\Omega_N}\lambda_{shedding,i}\cdot\sum_{t}^{T}P^{t}_{shedding,i}\right\} \quad (11)$$

where μ_{ij} is a binary variable, if the line (i, j) is faulty due to the hurricane, μ_{ij} equals 1. Otherwise, μ_{ij} equals 0.

In the Min-Max-Min optimization model, the first-stage constraints, second-stage constraints, and uncertain variables are presented in the following sections.

A. FIRST-STAGE CONSTRAINTS

The first-stage model co-optimizes the pre-allocation of MEGs and the network topology of the DS, which subjects to the following constraints.

(1) Pre-positioning MEGs constraints.

$$\sum_{i}^{\Omega_{Nm}}\alpha_{m,i}=1,\quad \forall m\in M \quad (12)$$

$$\sum_{m}^{M}\alpha_{m,i}\le CAP_i,\quad \forall i\in\Omega_N \quad (13)$$

Constraint (12) enforces that each MEG can only be pre-assigned to one candidate waiting node. Constraint (13) restricts the capacity of MEGs connected to a node. Here, CAP_i is allowed capacity of MEGs connected to node i.

(2) DS topology reconfiguration constraints. To meet the radial topology requirements of the distribution network, we construct the following constraints based on the fictitious network method [28].

$$\sum_{(i,j)\in\Omega_L}\beta^{pri}_{ij}=n_{\text{node}}-n_{\text{sub}} \quad (14)$$

$$\sum_{(j,i)\in\Omega_L}f^{fic}_{org,ji}-\sum_{(i,j)\in\Omega_L}f^{fic}_{org,ij}=f^{load}_{org,i},\quad \forall i\in\Omega_N\setminus\Omega_{sub} \quad (15)$$

$$\sum_{(i.j)\in\Omega_L}f^{fic}_{org,ij}-\sum_{(j,i)\in\Omega_L}f^{fic}_{org,ji}=f^{source}_{org,i},\quad \forall i\in\Omega_{sub} \quad (16)$$

$$-\beta^{pri}_{ij}\cdot K_1\le f^{fic}_{org,ij}\le\beta^{pri}_{ij}\cdot K_1,\quad \forall(i,j)\in\Omega_L \quad (17)$$

$$f^{source}_{org,i}\ge 1,\quad \forall i\in\Omega_{sub} \quad (18)$$

Constraints (14)-(18) guarantee that the distribution network satisfies two conditions: 1) there is only one substation in each network; 2) each load node belongs to only one network. Constraint (14) limits the number of closed branches to meet the condition 1); Constraints (15) and (16) guarantee the fictitious flow balance at all load nodes and substation nodes; Constraint (17) limits the fictitious flow on disconnected lines to be zero; Constraint (18) restricts the amount of fictitious flow out of a substation node, which prevents the single substation node from forming an island. Here, n_{node} and n_{sub} are the numbers of all nodes and substation nodes in the distribution network; K_1 is a sufficiently large positive coefficient.

(3) DS operation constraints.

$$\sum_{(j,i)\in\Omega_L}p^{t}_{org,ji}-\sum_{(i,j)\in\Omega_L}p^{t}_{org,ij}=p^{t}_{org,i}-P^{t}_{org,i},\ \forall i\in\Omega_N,\forall t\in T \quad (19)$$

$$\sum_{(j,i)\in\Omega_L}q^{t}_{org,ji}-\sum_{(i,j)\in\Omega_L}q^{t}_{org,ij}=q^{t}_{org,i}-Q^{t}_{org,i},\forall i\in\Omega_N,\ \forall t\in T \quad (20)$$

$$\left(p^{t}_{org,ij}\right)^2+\left(q^{t}_{org,ij}\right)^2\le\beta^{pri}_{ij}\left(s^{\max}_{ij}\right)^2,\forall(i,j)\in\Omega_L,\forall t\in T \quad (21)$$

$$\left(V^{\min}_{i}\right)^2\le\left(v^{t}_{org,i}\right)^2\le\left(V^{\max}_{i}\right)^2,\ \forall i\in\Omega_N,\forall t\in T \quad (22)$$

$$\left(v^{t}_{org,i}\right)^2-\left(v^{t}_{org,j}\right)^2\le\left(1-\beta^{pri}_{ij}\right)\cdot K_2+2\left(p^{t}_{org,ij}r_{ij}+q^{t}_{org,ij}x_{ij}\right),\ \forall(i,j)\in\Omega_L,\forall t\in T \quad (23)$$

$$\left(v^{t}_{org,i}\right)^2-\left(v^{t}_{org,j}\right)^2\ge\left(\beta^{pri}_{ij}-1\right)\cdot K_2+2\left(p^{t}_{org,ij}r_{ij}+q^{t}_{org,ij}x_{ij}\right),\ \forall(i,j)\in\Omega_L,\forall t\in T \quad (24)$$

$$0\le P^{t}_{org,i}\le\sum_{m}^{M}\alpha_{m,i}\cdot P^{\max}_{m},\quad \forall i\in\Omega_{Nm},\forall t\in T \quad (25)$$

$$0\le Q^{t}_{org,i}\le\sum_{m}^{M}\alpha_{m,i}\cdot Q^{\max}_{m},\quad \forall i\in\Omega_{Nm},\forall t\in T \quad (26)$$

Equations (19)-(20) represent the active and reactive power balance at each node in the distribution network. Here, we think that advanced balancing devices installed in the DS could avoid three-phase unbalance problems. Constraint (21) limits the apparent power capacity of each line. Constraint (22) determines the range of voltage fluctuation at each node. Constraints (23) and (24) indicate the voltage of each line based on the DistFlow model. Constraints (21)-(24) are nonlinear, which could be linearized via using the approach proposed in [29]. Constraints (25) and (26) declare that the injected active and reactive power at the node connected to the MEGs is limited by the maximum capacity of the MEGs. Here, $v^{t}_{org,i}$ is the voltage value of node i at time t before the hurricane; K_2 is a sufficiently large positive coefficient.

B. UNCERTAINTY

In this study, the impact of hurricane disaster on power infrastructure is regarded as uncertain, represented by functional states of transmission corridors. Based on the failure probability model of transmission corridors constructed in Section II, the uncertainty set of power network vulnerability during the extreme event is modeled as follows [22]:

This article has been accepted for publication in a future issue of this journal, but has not been fully edited. Content may change prior to final publication. Citation information: DOI 10.1109/ACCESS.2021.3102497, IEEE Access

$$U=\left\{\mu_{ij}\left|\frac{1}{2}\sum_{(i,j)\in\Omega_L}\left(-\log_2 p_{line,ij}\right)\mu_{ij}\le\Gamma\right.\right\} \tag{27}$$

where Γ is the uncertainty budget of the failure of the network. Under the given failure probability of the lines, a larger value of Γ means that the uncertainty set contains more faulty transmission corridors damaged by the hurricane. In this situation, the optimization model based on the uncertainty set with large Γ would be more conservative. Therefore, the conservative level of the proposed optimization approach could be adjusted via setting the value of the uncertainty budget Γ. This solves the problem that the application of traditional robust schemes is poor due to the high conservative level.

C. SECOND-STAGE CONSTRAINTS

The second-stage model co-optimizes supply-side and demand-side resources to improve the recovery of post-disaster DS's loads, which subjects to the following constraints.

(1) Post-disaster MEGs dispatch constraints.

$$\sum_{i}^{\Omega_{Nm}}\delta_{m,i}\le 1,\quad \forall m\in M \tag{28}$$

$$0\le p_{m,out}^{t}\le\sum_{i}^{\Omega_N}\delta_{m,i}\cdot P_m^{\max},\quad \forall m\in M,\forall t\in T \tag{29}$$

$$0\le q_{m,out}^{t}\le\sum_{i}^{\Omega_N}\delta_{m,i}\cdot Q_m^{\max},\quad \forall m\in M,\forall t\in T \tag{30}$$

Constraint (28) indicates that each MEG can only be sent to at most one of its candidate nodes from the pre-positioning location of the first stage. Constraints (29) and (30) declare the boundary of output active and reactive power of each MEG.

(2) Constraints of post-disaster DS topology reconfiguration. After the extreme disaster, some lines in the power network would break off. To continue to supply electrical energy to consumers, the power network's topological connection structure needs to be changed via remote-controlled switches. Note that the switch sequence generation and the process of the network topology reconstruction are beyond the scope of this work. Interested readers may refer to [31-33], etc. The constraints of topology reconfiguration of post-disaster DS are described as follows:

$$\beta_{ij}^{post}\le\left(1-\mu_{ij}\right)\cdot\left(l_{ij}+\beta_{ij}^{pri}\right),\forall\left(i,j\right)\in\Omega_L \tag{31}$$

$$\beta_{ij}^{post}\ge\left(1-\mu_{ij}\right)\cdot\left(-l_{ij}+\beta_{ij}^{pri}\right),\forall\left(i,j\right)\in\Omega_L \tag{32}$$

$$\sum_{(i,j)\in\Omega_L}\beta_{ij}^{post}=n_{\text{node}}-n_{\text{island}} \tag{33}$$

$$\sum_{(j,i)\in\Omega_L}f_{post,ji}^{fic}-\sum_{(i,j)\in\Omega_L}f_{post,ij}^{fic}=f_{post,i}^{load},\quad\forall i\in\Omega_N\setminus\Omega_{fs} \tag{34}$$

$$\sum_{(i.j)\in\Omega_L}f_{post,ij}^{fic}-\sum_{(j,i)\in\Omega_L}f_{post,ji}^{fic}=f_{post,i}^{source},\quad\forall i\in\Omega_{fs} \tag{35}$$

$$-\beta_{ij}^{post}\cdot K_1\le f_{post,ij}^{fic}\le\beta_{ij}^{post}\cdot K_1,\quad\forall\left(i,j\right)\in\Omega_L \tag{36}$$

Constraints (31) and (32) indicate that the transmission corridors are open if they are broken, and the undamaged lines remain in their pre-disaster status if they do not have the remote-controlled switches. Like constraints (14)-(17) illustrated in Section III.B, constraints (33)-(36) ensure that the reconstructed distribution network still maintains radial topology. Wherein constraint (33) declares the relationship between the number of closed branches and the number of islands after the disaster. Here, n_{island} is the number of all islands formed after the extreme disaster.

(3) Post-disaster DS operation constraints.

$$\sum_{(j,i)\in\Omega_L}p_{ji}^{t}-\sum_{(i,j)\in\Omega_L}p_{ij}^{t}=p_i^t-P_i^t,\forall i\in\Omega_N,\forall t\in T \tag{37}$$

$$\sum_{(j,i)\in\Omega_L}q_{ji}^{t}-\sum_{(i,j)\in\Omega_L}q_{ij}^{t}=q_i^t-Q_i^t,\forall i\in\Omega_N,\forall t\in T \tag{38}$$

$$\left(p_{ij}^{t}\right)^2+\left(q_{ij}^{t}\right)^2\le\beta_{ij}^{post}\cdot\left(s_{ij}^{\max}\right)^2,\forall\left(i,j\right)\in\Omega_L,\forall t\in T \tag{39}$$

$$\left(v_i^t\right)^2-\left(v_j^t\right)^2\le\left(1-\beta_{ij}^{post}\right)\cdot K_2+2\left(p_{ij}^{t}\cdot r_{ij}+q_{ij}^{t}\cdot x_{ij}\right),\quad\forall\left(i,j\right)\in\Omega_L,\forall t\in T \tag{40}$$

$$\left(v_i^t\right)^2-\left(v_j^t\right)^2\ge\left(\beta_{ij}^{post}-1\right)\cdot K_2+2\left(p_{ij}^{t}\cdot r_{ij}+q_{ij}^{t}\cdot x_{ij}\right),\quad\forall\left(i,j\right)\in\Omega_L,\forall t\in T \tag{41}$$

$$\left(V_i^{\min}\right)^2\le\left(v_i^t\right)^2\le\left(V_i^{\max}\right)^2,\forall i\in\Omega_N,\forall t\in T \tag{42}$$

$$P_i^t=\sum_{m}^{M}\delta_{m,i}\cdot p_{m,out}^{t},\forall i\in\bigcup_{m\in M}\Omega_{Nm},\forall t\in T \tag{43}$$

$$Q_i^t=\sum_{m}^{M}\delta_{m,i}\cdot q_{m,out}^{t},\forall i\in\bigcup_{m\in M}\Omega_{Nm},\forall t\in T \tag{44}$$

Constraints (37)-(44), similar to constraints (19)-(26) constructed in Section III.B, declare the operational requirements of post-disaster DS. Here, v_i^t is the voltage value of node i at time t after the hurricane. Constraints (39)-(44) are nonlinear, which could be linearized via using the approach proposed in [30, 34].

(4) Operational constraints of energy coupling equipment. Each PC mainly contains two types of energy conversion devices: CHP units and EBs, in this paper. Wherein CHP units consume natural gas to provide electrical and thermal energy for the end-users. And EBs generate thermal power to meet the heating demand. The operational constraints of CHP units and EBs are presented as follows [30, 35]:

$$L_{out,k}^{CHP,e}=\eta_{me,k}^{CHP}M_{in,k}^{CHP} \tag{45}$$

$$L_{out,k}^{CHP,h}=\eta_{mh,k}^{CHP}M_{in,k}^{CHP} \tag{46}$$

$$L_{out,k}^{EB,h}=\eta_{eh,k}^{EB}M_{in,k}^{EB} \tag{47}$$

$$L_{out,k,\min}^{CHP}\le L_{out,k}^{CHP}\le L_{out,k,\max}^{CHP} \tag{48}$$

$$L_{out,k,\min}^{EB}\le L_{out,k}^{EB}\le L_{out,k,\max}^{EB} \tag{49}$$

Constraints (45)-(47) describe the relationship between the output and input power of CHP units and EBs. Constraints (48) and (49) restrict the range of output power of the CHP units and EBs.

(5) DR constraints. The energy consumers in PCs participate in the DR program to help the DS further enhance the post-disaster load restoration capacity based on the limited power supply resources. According to the operation characteristics of energy consumption devices, the load devices can be divided into fixed loads (FLs), non-interruptible shiftable loads (NISLs), interruptible shiftable loads (ISLs). This paper focuses on the allocation schemes for resisting the extreme disaster by implementing the DR programs. In this case, we construct the directly controlled load model based on the power consumption characteristics of the load devices, which is more suitable for the emergency.

FLs include important load equipment and uncontrollable load equipment. The working time and operation cycle cannot be adjusted arbitrarily, such as lighting, refrigerator, and elevator. The mathematical model of FLs is shown as follows:

$$\begin{cases} P_{fl,a}^{t} = D_{fl,a}^{t}, & \forall t \in \left[t_{ope,a}^{start}, t_{ope,a}^{end} \right] \\ P_{fl,a}^{t} = 0, & \forall t \notin \left[t_{ope,a}^{start}, t_{ope,a}^{end} \right] \end{cases} \tag{50}$$

where $P_{fl,a}^{t}$ represents the power consumption of FL a at time t; $D_{fl,a}^{t}$ represents the electrical power of FL a at time t; $[t_{ope,a}^{start}, t_{ope,a}^{end}]$ is the operation time interval of FL a.

For NISLs, the start time of devices could be adjusted according to the users' demand. However, once the load equipment starts to run, it needs to work continuously for a period of time and cannot be interrupted. Specifically, washing machines, dryers, grinders, and so on all belong to NISLs. The mathematical model of NISLs is described as follows:

$$\begin{cases} P_{nisl,a}^{t} = D_{nisl,a}, & t_{a,s} \le t \le t_{a,s} + \Delta T_a \\ P_{nisl,a}^{t} = 0, & t < t_{a,s} \ or \ t > t_{a,s} + \Delta T_a \end{cases} \tag{51}$$

$$\omega_{sta,a} \le t_{a,s} \le \omega_{end,a} \tag{52}$$

$$\omega_{sta,a} \le t_{a,s} + \Delta T_a \le \omega_{end,a} \tag{53}$$

$$\sum_{t=\omega_{sta,a}}^{\omega_{end,a}} P_{nisl,a}^{t} = D_{nisl,a}^{total} \tag{54}$$

where $D_{nisl,a}^{t}$ represents the electrical power of NISL a at time t; $t_{a,s}$ is the start time of NISL a; ΔT_a is the time period for NISL a to complete the work; $[\omega_{sta,a}, \omega_{end,a}]$ is the schedulable time range of NISL a; $D_{nisl,a}^{total}$ is the all power required by NISL a to complete the work.

For ISLs, the operation time is flexible. The start time of ISL devices could be adjusted, and the operation of ISL equipment can be interrupted at any time. For example, air conditioners and hybrid electric vehicles are ISLs [36]. The mathematical model of NISLs is built as follows:

$$\begin{cases} D_{isl,a}^{\min} \le P_{isl,a}^{t} \le D_{isl,a}^{\max}, & \omega_{sta,a} \le t \le \omega_{end,a} \\ P_{isl,a}^{t} = 0, & t < \omega_{sta,a} \ or \ t > \omega_{end,a} \end{cases} \tag{55}$$

$$P_{isl,a}^{t} = \upsilon_a^t D_{isl,a}^{\max} + (1 - \upsilon_a^t) D_{isl,a}^{\min}, \ \forall t \in \left[\omega_{sta,a}, \omega_{end,a} \right] \tag{56}$$

$$\sum_{t=\omega_{sta,a}}^{\omega_{end,a}} P_{isl,a}^{t} = D_{isl,a}^{total} \tag{57}$$

where $D_{isl,a}^{max}$ and $D_{isl,a}^{min}$ are the upper and lower limits of operation power of ISL a respectively; υ_a^t is a binary variable. If ISL device a is operating, υ_a^t equals 1; otherwise, υ_a^t equals 0. $D_{isl,a}^{total}$ is all power required by ISL a to complete the work.

(6) Energy conservation constraints. For traditional load nodes of the DS, the electrical energy balance relationship is formulated as follows:

$$P_{shedding,i}^{t} = p_{org,i}^{t} - p_i^t, \quad \forall t \in T, \forall i \in \Omega_N \setminus \Omega_{pro} \tag{58}$$

In PCs, the energy load demand mainly includes electrical load and thermal load. Based on this, the electrical and thermal energy balance relationships in each PC are respectively shown as follows:

$$\begin{aligned} &\sum_{m}^{M} \delta_{m,i}^{t} \cdot p_{m,out}^{t} + p_{pv,i}^{t} + \sum_{k}^{\Omega_{CHP}} L_{out,k,i}^{CHP,e,t} + P_{shedding,i}^{t} \\ &= \sum_{k}^{\Omega_{EB}} M_{in,k,i}^{EB,e,t} + \sum_{a}^{\Omega_{fl}} P_{fl,a,i}^{t} + \sum_{a}^{\Omega_{nisl}} P_{nisl,a,i}^{t} + \sum_{a}^{\Omega_{isl}} P_{isl,a,i}^{t}, \\ &\forall t \in T, \ \forall i \in \Omega_{pro} \end{aligned} \tag{59}$$

$$\sum_{k}^{\Omega_{CHP}} L_{out,k,i}^{CHP,h,t} + \sum_{k}^{\Omega_{EB}} L_{out,k,i}^{EB,h,t} \ge \sum_{a}^{\Omega_{HL}} P_{Load,a,i}^{h,t}, \forall t \in T, \forall i \in \Omega_{pro} \tag{60}$$

where $p_{pv,i}^{t}$ is the power output of PV in the PC i at time t.

It is worth mentioning that the proposed approach can be applied to larger scale systems. Because the size of the distribution system mainly affects the number of sub-network formed due to system reconfiguration after the extreme disasters. And compared with the smaller scale power system, the larger scale system mainly brings about changes in the number and capacity of mobile emergency generators, energy coupling units, renewable energy resources, and controllable loads. This would not influence the structure of the contructed model. Therefore, the proposed approach has scalable.

D. SOLUTION METHODOLOGY

In this paper, we adopt the C&CG algorithm to solve the proposed two-stage RO model. In the C&CG approach, the two-stage problem needs to be decomposed into a master problem and sub-problem. For the sake of clarity, the master problem and sub-problem can be expressed in compact form, shown in (61) and (62), respectively.

$$\begin{aligned} &\min_{\phi^f \in \Phi^f} \eta_{C\&CG} \\ &s.t. \ \eta_{C\&CG} \ge C_0^T u + W_0^T \phi^s \\ &\quad \Lambda_1^T \phi^f + C_1^T u + W_1^T \phi^s = c_1 \\ &\quad \Lambda_2^T \phi^f + C_2^T u + W_2^T \phi^s \le c_2 \end{aligned} \tag{61}$$

where ϕ^f, u, ϕ^s are first-stage decision variables ($\alpha_{m,i}$, $f_{org,ij}^{fic}$, β_{ij}^{pri}, $f_{org,i}^{source}$), uncertainty variables (μ_{ij}), and second stage decision variables ($\delta_{m,i}^{t}$, $p_{m,out}^{t}$, p_i^t, $L_{out,k,i}^{CHP,e,t}$, $M_{in,k,i}^{EB}$, $P_{nisl,a}^{t}$, $P_{isl,a}^{t}$) respectively. $\eta_{C\&CG}$ is the objective function value of the subproblem. Λ, C, W, c_1, c_2 are the coefficients of variables and constants in constraints (12)-(60).

This article has been accepted for publication in a future issue of this journal, but has not been fully edited. Content may change prior to final publication. Citation information: DOI 10.1109/ACCESS.2021.3102497, IEEE Access

$$\max_{u\in U}\min_{\phi^s\in\Phi^s} C_0^T u + W_0^T \phi^s$$
$$s.t.\ A_1^T \phi^{f*} + C_1^T u + W_1^T \phi^s = c_1 \quad (62)$$
$$A_2^T \phi^{f*} + C_2^T u + W_2^T \phi^s \le c_2$$

where U is the feasible regions of u. The above sub-problem, a max-min problem, cannot be solved directly, which needs to be transformed into a mixed-integer linear optimization problem based on duality theory [37] and the Big-M method as follows:

$$\max_{u,\vartheta,\pi} C_0^T u + \left(c_1 - A_1^T \phi^{f*} - C_1^T u\right)^T \vartheta + \left(A_2^T \phi^{f*} + C_2^T u - c_2\right)^T \pi$$
$$s.t.\ A_1^T \phi^{f*} + C_2^T u + W_1^T \phi^s = c_1$$
$$W_0^T + \vartheta^T W_1 + \pi^T W_2 = 0 \quad (63)$$
$$0 \le c_2 - A_2^T \phi^{f*} - C_2^T u - W_2^T \phi^s \le M \cdot \xi$$
$$0 \le \pi \le K_3 \cdot (1-\xi)$$
$$\vartheta \ge 0,\ \ \pi \ge 0$$

where ϑ and π are dual variables of the max-min problem (62); M is a large value in the Big-M method, and the value of ξ is 1 or 0.

Based on the above models, the optimal solution of the proposed two-stage RO problem will be obtained via iteratively solving the master problem (61) and sub-problem (63), and the details could refer to [35, 38].

V. CASE STUDY

A. TEST DATA

The effectiveness of the proposed approach for the improvement of load restoration in DS with multiple energy resources is tested on an IEEE 123-bus test system [39], which has 85 load nodes, 118 transmission corridors. In this system, three PCs are connected with the DS at nodes 14, 18, and 32. The total PV production profile, electric loads, and heat loads demand data of the three PCs are shown in Fig.3, and the parameters of CHP units and EBs [40] are respectively listed in Table.I. Besides, we consider 2 MEGs with 50kW capacity and 3 MEGs with 200 kW capacity equipped in the DS.

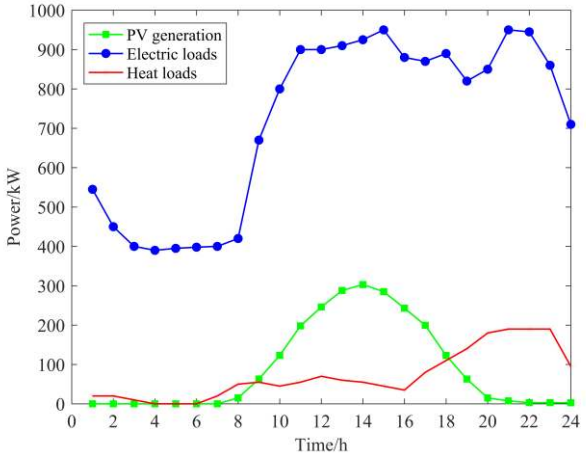

FIGURE 3. The total PV production profile, electric loads, and heat loads demand of the three PCs.

TABLE I
PARAMETERS OF CHP UNITS AND EBS IN EACH PC

PC nodes	Facility	Number	Parameter	Value
18	CHP units	3	$L_{out,max}^{CHP,e}$	50kW
			$L_{out,min}^{CHP,e}$	0kW
			η_{ge}^{CHP}	0.3
			η_{gh}^{CHP}	0.4
	EBs	1	$M_{in,max}^{EB,e}$	20kW
			$M_{in,min}^{EB,e}$	0kW
			η_{eh}^{EB}	0.9
14	CHP units	5	$L_{out,max}^{CHP,e}$	50kW
			$L_{out,min}^{CHP,e}$	0kW
			η_{ge}^{CHP}	0.3
			η_{gh}^{CHP}	0.4
	EBs	1	$M_{in,max}^{EB,e}$	20kW
			$M_{in,min}^{EB,e}$	0kW
			η_{eh}^{EB}	0.9
32	CHP units	4	$L_{out,max}^{CHP,e}$	100kW
			$L_{out,min}^{CHP,e}$	0kW
			η_{ge}^{CHP}	0.3
			η_{gh}^{CHP}	0.4
	EBs	1	$M_{in,max}^{EB,e}$	30kW
			$M_{in,min}^{EB,e}$	0kW
			η_{eh}^{EB}	0.9

In addition, to calculate the wind speed at each node in DS, we take node 13 as the origin to establish a rectangular coordinate system, while assuming that the coordinate of the hurricane eye is (17, 17) in the rectangular coordinate system. Here we consider extreme wind profiles characterized in reference [23]. Based on all nodal coordinates of the studied system and the location of the hurricane eye, the wind speed of all nodes can be calculated via (1). Moreover, we adopt fragility curves of the components that are 0, 10, 30, and 50 years old [41] to study the effect of components degradation on the failure probability of transmission corridors during the disturbance event, illustrated in Fig.4. In this simulation, the duration of the hurricane event progress (Phase II) is known as 2 hours. The data for the operation time of the switch is based on [23].

To assess the resilience of DS, we adopt risk-based quantitative measures proposed in [23], including value-at-risk (*VaRα*) and conditional-value-at risk (*CVaRα*). The calculation method of *VaRα* and *CVaRα* can be found in reference [23]. And like reference [23], we also use loss in energy to measure the operational resilience of the DS during the hurricane disaster.

This article has been accepted for publication in a future issue of this journal, but has not been fully edited. Content may change prior to final publication. Citation information: DOI 10.1109/ACCESS.2021.3102497, IEEE Access

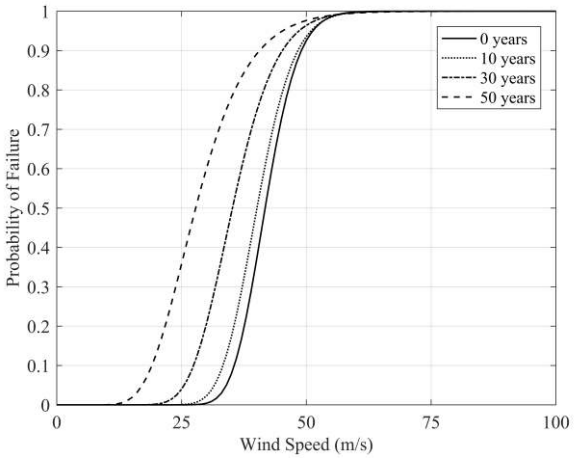

FIGURE 4. Fragility curves of components that are 0, 10, 30, and 50 years old.

B. SIMULATION RESULTS

1) EFFECTIVENESS OF THE Z-NUMBER MODELLING APPROACH

In this paper, we propose a Z-number-based method to estimate the failure probability of components under given wind speed, which considers the effect of aging of components and the reliability/credibility of the fragility curve. To evaluate the effectiveness of the proposed approach, we compared the failure probability of all transmission corridors obtained via the conventional method (one single fragility curve) and proposed Z-number-based method with considering the degradation of poles, represented by three scenarios as shown in Table. II.

TABLE II
SCENARIO SETTINGS FOR VALIDATION OF Z-NUMBER BASED COMPONENTS FAILURE MODEL

Scenarios	Incorporating aging	Method	Credibility of fragility curve	A	B
1	×	Conventional method	-	-	-
2	√	Z-number	Low	$(p^0_{line,ij}, p^{10}_{line,ij}, p^{30}_{line,ij}, p^{50}_{line,ij})$	(0.5,0.6,0.7)
3	√	Z-number	High	$(p^0_{line,ij}, p^{10}_{line,ij}, p^{30}_{line,ij}, p^{50}_{line,ij})$	(0.8,0.9,1)

Specifically, in Scenarios 1, we consider that the failure probability of components calculated through one single empirical fragility curve (the 0 years curve in Fig.4) is completely credible, and the degradation of components is not considered. Compared with Scenarios 1, in Scenarios 2 and 3, both the credibility of fragility curves and the aging of components are considered by using the Z-number-based fragility modeling method. Wherein the credibility of fragility curves is classified as low and high, reflected via fuzzy number B in the Z-number model. And $p^0_{line,ij}$, $p^{10}_{line,ij}$, $p^{30}_{line,ij}$, and $p^{50}_{line,ij}$ represent the failure probability of each transmission line that are 0, 10, 30, and 50 years old, which is calculated based on the corresponding fragility curves in Fig.4.

Here, we take branch 35-36 as an example. And its failure probability affected by different wind speeds is calculated based on the above three scenarios, illustrated in Fig.5.

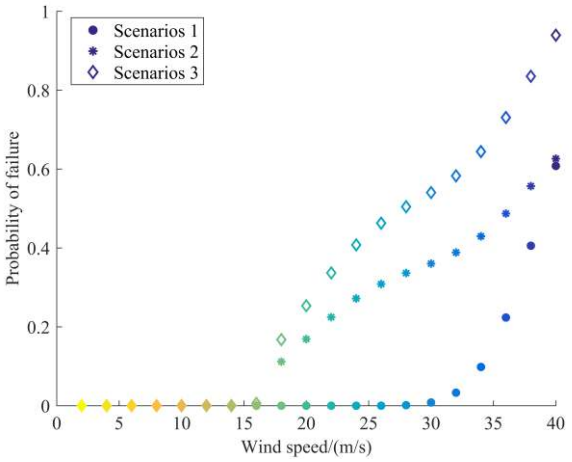

FIGURE 5. The failure probability of branch 35-36 calculated in the proposed three scenarios.

As observed, as the wind speed grows, the failure probability of branch 35-36 obtained by conventional method and Z-number method become greater. And failure probability under the same wind speed calculated by the three scenarios is quite different. Specifically, the results of one single fragility (Scenario 1) are much lower than the results of the Z-number method (Scenario 2 and 3). This indicates that, the aging of components and credibility of fragility curves have a significant effect on modeling grid fragility. And the component failure probability model built by the conventional method is more conservative for evaluating the influence of hurricanes on energy infrastructure. Besides, under the same wind speed, the failure probability obtained via Scenarios 3 is larger than that via Scenarios 1. This suggests that, the calculated failure probability would increase if the degradation of components is considered, which is consistent with reality. Thus, it is necessary to consider the degradation of components and credibility of fragility curves when constructing the vulnerability model of the power network. And Z-number-based modeling method could provide a more realistic and comprehensive estimation of the failure probability of the power network caused by extreme disasters.

2) EFFECTIVENESS OF THE PROPOSED ELR APPROACH

To illustrate the effectiveness of the proposed DS resilience improvement approach, three cases with different load restoration resources and a deterministic case have been defined in Table. III, and a comparative analysis is conducted based on these cases.

This article has been accepted for publication in a future issue of this journal, but has not been fully edited. Content may change prior to final publication. Citation information: DOI 10.1109/ACCESS.2021.3102497, IEEE Access

TABLE III
SCENARIO SETTINGS FOR VALIDATION OF ELR STRATEGY

Case	Distributed energy resources	DR	Optimization method
1	×	×	RO
2	√	×	Two-stage RO
3	√	√	Two-stage RO
4	√	√	Deterministic

Specifically, in Case 1, we consider no available energy supply and demand resources for the ELR after the hurricane. Thus, Case 1 is the base case, which shows the post-disaster DS's load loss without extra energy resources for load restoration. Compared with Case 1, the distributed energy resources, including MEGs, CHP units, EBs and PV sources, and DR programs, are considered in Case 2, Case 3, and Case 4. And Case 4 adopts deterministic optimization without considering the uncertainties. Besides, the Z-number-based fragility model with high credibility of the fragility curve is adopted in the three cases to construct the uncertain set of the transmission corridors' functional states under the hurricane.

Based on the above cases, the load loss and performance loss of DS caused by the hurricane are calculated with different values of failure uncertainty budget Γ, shown in Fig.6-7.

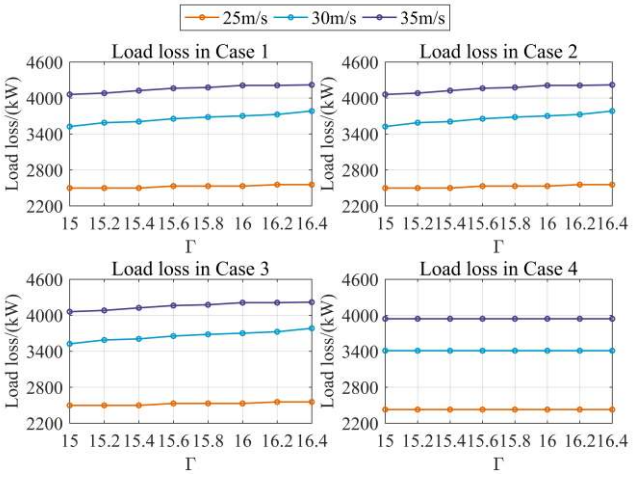

FIGURE 6. The load loss of the DS with different values of failure uncertainty budget.

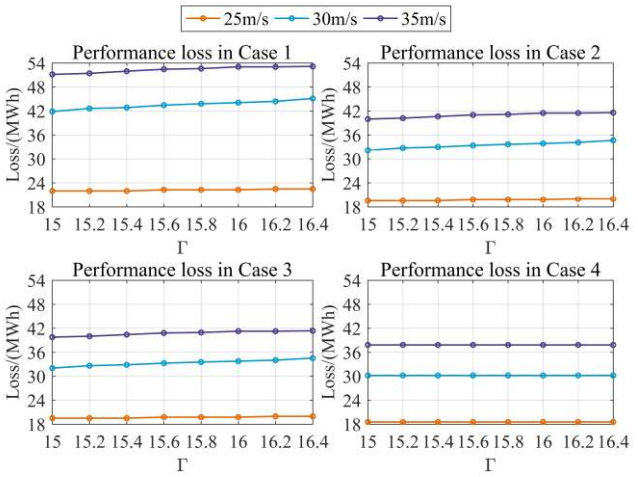

FIGURE 7. The performance loss of DS with different values of failure uncertainty budget.

It can be seen from Fig.6 that, the DS load loss in Case 1, 2, and 3 are the same, but the DS load loss in Case 4 is smaller than that in Case 1, 2 and 3. This is because, Case 1, 2, and 3 all adopt robust optimization, and the resilience improvement methods based on resource allocation (adopted in Case 2 and 3) do not reduce the initial impact of the hurricane on the power system. Besides, the robust optimization method considers the worst situation realization of the uncertainty (the damage scenario of the DS in this paper), which causes the larger load loss in Case 1, 2, and 3. Besides, the deterministic optimization does not consider the uncertainty, so the DS load loss in Case 4 is unchanged with different failure uncertainty budget Γ.

It can be seen from Fig.6-7 that, under the same wind speed, the trends of the DS performance loss in the three cases are roughly the same as the trends of the DS load loss with the increase of the failure uncertainty budget Γ. And as the failure uncertainty budget Γ and wind speed get larger, the load loss and performance loss of DS increase, which means that the operational performance of DS declines. The reason is that, parameter Γ limits the maximum number of faulty lines, and represents the impact intensity of disaster on the distribution network. Besides, subjected to the same wind intensity, the performance loss in Case 2 and 3 is smaller than those in Case 1. This indicates that, distributed energy resources and DR programs contribute to load restoration of post-disaster DS. Last but not least, consideration of the worst scenario in robust optimization results in the larger performance loss in Case 3, compared with deterministic optimization (Case 4). And like load loss, the performance loss in Case 4 stays the same for different failure uncertainty budget Γ.

To further explore the effect of the proposed resource allocation method on DS resilience, $VaR\alpha$ and $CVaR\alpha$ of the DS in the above four cases are calculated to quantify the resilience of DS during the hurricane.

To obtain the $VaR\alpha$ and $CVaR$, we calculate the DS performance loss for each wind speed, and map it into the

This article has been accepted for publication in a future issue of this journal, but has not been fully edited. Content may change prior to final publication. Citation information: DOI 10.1109/ACCESS.2021.3102497, IEEE Access

probability density function (PDF) of wind speeds to form probabilistic performance loss of the DS [23], shown in Fig.8.

Based on this, the *VaRα* and *CVaR* of three cases can be determined, shown in Table.IV Note that, the failure uncertainty budget of 15 is considered for simulation while calculating the probabilistic performance loss, *VaRα*, and *CVaRα* of the DS in the four cases.

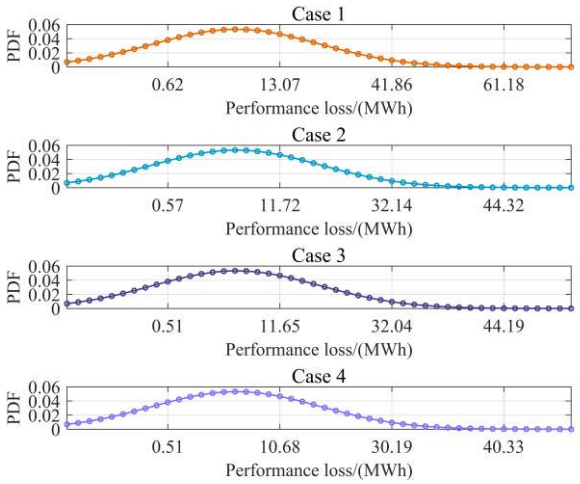

FIGURE 8. The probabilistic performance loss of DS in the four cases.

TABLE IV
VAR AND *CVAR* FOR DIFFERENT CASES WITH α=95%

Case	*VaRα*(MWh)		*CVaRα*(MWh)	
	This paper	Reference [23]	This paper	Reference [23]
1	40.96	61.10	47.78	68.22
2	31.67	52.53	35.54	56.73
3	31.58	-	34.87	-
4	29.94	-	32.66	-

It can be observed from Table. IV that, the *VaRα* and *CVaR* of Case 1 are larger than that of Case 2, 3, and 4. This indicates that, distributed energy resources and DR programs (Case 2 and 3) are helpful for boosting the DS operational resilience during the hurricane disaster. And compare with distributed energy resources, the effect of DR programs on DS resilience improvement is smaller. This is because, we only consider the DR programs in PCs in this paper. And the controllable loads are very small compared to the whole loads in the DS. Hence, to enhance the effect of DR, the DS could encourage more customers to participate in the DR programs by taking some incentives.

Besides, to confirm the validity of the obtained calculation results, we compare the above simulation results with reference [23], illustrated in Table.IV It can be observed that, the values of *VaRα* and *CVaR* calculated in this paper are smaller than that in reference [23]. This is because, the components failure probability model adopted in this paper is different from that in reference [23]. Based on this, the failure probability of the same transmission lines influenced by the same wind intensity would be different. What's more, this paper uses a different damage scenarios modeling method for particular wind speed from reference [23]. This is why, although these two papers adopt the same wind profile, DSs in the two papers have different levels of damage. And then, the DS performance loss, *VaRα*, and *CVaR* obtained in the two papers are different.

3) ECONOMIC ANALYSIS OF RESOURCE ALLOCATION PLAN

Based on the cases defined in Table. III, the load shedding costs of DS are optimized as shown in Table. V. Note that, the failure uncertainty budget of 15 and the wind speed of 30m/s are considered for the simulation in this section.

TABLE V
VARIOUS COSTS OF POWER DSS IN DIFFERENT CASES

Case	1	2	3	4
Shedding costs (￥)	1598360.99	1078823.43	1014251.42	955688.21

It can be seen from Table. V, load shedding cost of Case 3 is greater than Case 4 since the robust optimization determines the optimal scheme considering the worst scenario of the hurricane damage. And the DS's load shedding cost without distributed energy resources and DR (Case 1) is significantly larger than that of the DS in Case 2 and 3. As the DS is equipped with multi-energy supply resources, including MEGs, CHP units, EBs, and PV generators in Case 2, the load loss cost of DS is reduced by about 519.37 thousand yuan. This indicates that, emergency energy supply resources and distributed energy supply resources contribute to the ELR of post-disaster DS. Besides the multi-energy supply resources in Case 2, implementation of the DR program in Case 3 achieves a further reduction in load shedding cost. Compared with Case 1, the reduced load loss cost of Case 3 is about 584.11 thousand yuan, which is 36.54% of the total load loss cost in Case 1 (without supply-side and demand-side resources for load restoration). Therefore, allocation of multi-energy supply resources and DR programs in a coordinated way is capable of effectively enhancing the load restoration of post-disaster DS and decreasing the economic losses of DS caused by disasters.

4) EFFECT OF DR

In this study, the electrical consumers in PCs participate in the DR program after the hurricane strikes to improve the load recovery. To confirm this effect, a comparative study is performed in this section, based on Case 2 and Case 3 created in Table. III considering the different configurations of load restoration resources.

In Case 2, the DS is equipped with CHP units, EBs, and PV generators at nodes 14, 18, and 32, and MEGs are allocated to different sub-network. But the DR resources are not taken into consideration. In Case 3, the configuration of energy supply resources are the same as the Case 2, and DR programs are implemented at the node 14, 18 and 32 (the three PCs).

Based on the above Cases 2 and 3, the electrical energy consumption of nodes 14, 18, and 32 is presented in Fig.9-14.

This article has been accepted for publication in a future issue of this journal, but has not been fully edited. Content may change prior to final publication. Citation information: DOI 10.1109/ACCESS.2021.3102497, IEEE Access

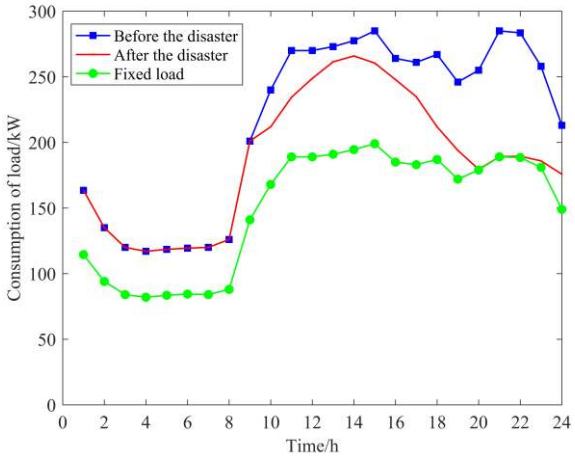

FIGURE 9. **Load consumption of the PC at node 14 in Case 2.**

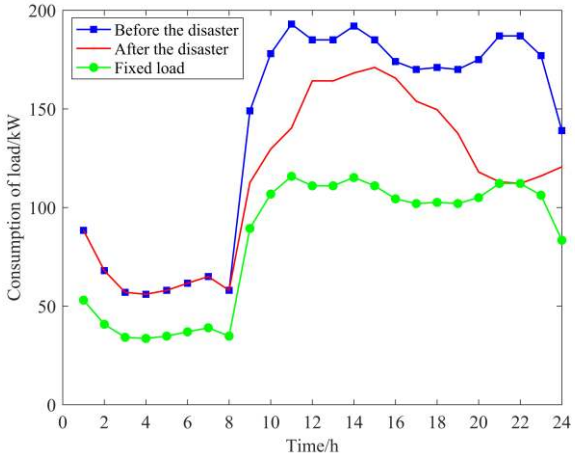

FIGURE 10. **Load consumption of the PC at node 18 in Case 2.**

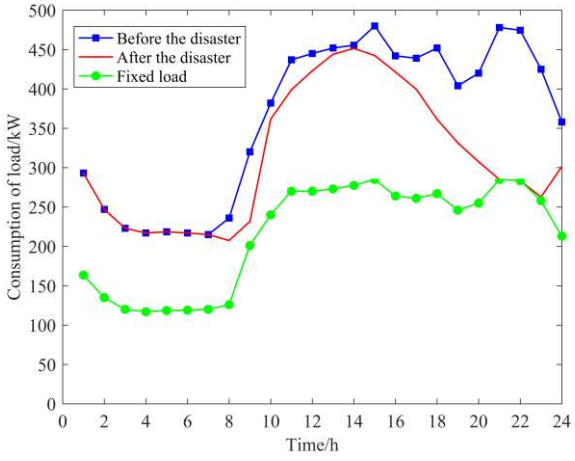

FIGURE 11. **Load consumption of the PC at node 32 in Case 2.**

Fig.9-11 show the load consumption of three PCs without implementing the DR program before and after the hurricane disaster (Case 2). It can be seen that, MEGs, CHP units, EBs, and PV generators can provide electrical energy to meet a part of the electrical demand of consumers after the partial transmission corridors are damaged by the hurricane disaster. And the FLs demand, mainly including critical loads and uncontrollable loads, could be fully satisfied through emergency energy supply sources after the hurricane. However, the electricity offered by the above emergency energy supply resources and distributed energy sources cannot fully meet all end users' power demands, and a part of the loads are still in a blackout due to the disaster. The reason is that the output power of the MEGs, CHP units, EBs, and PV sources are restricted, owing to the limitation of investment, operation, and maintenance cost of the additional power supply equipment. Thus, to fully restore the loads after the disaster, utilization of multi-energy supply resources, such as MEGs, CHP units, EBs, and PV generators, is insufficient.

To further improve the load restoration of post-disaster DS, in Case 3, the DR program is implemented in PCs connected to DS via nodes 14, 18, and 32.

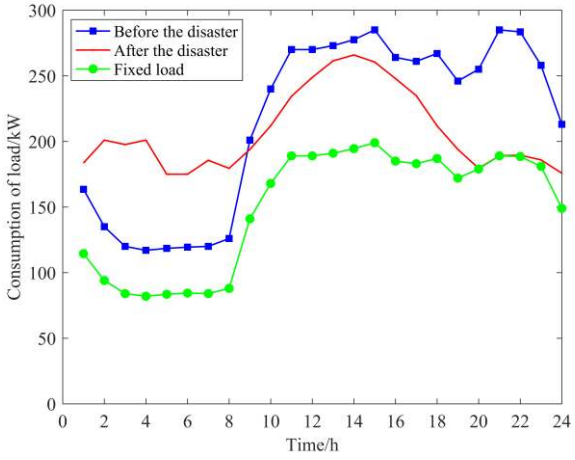

FIGURE 12. **Load consumption of the PC at node 14 in Case 3.**

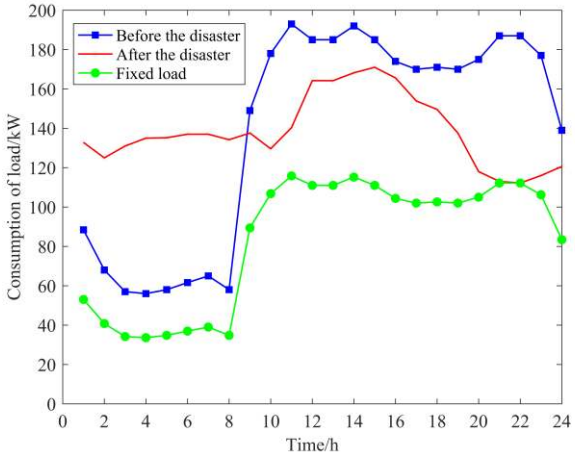

FIGURE 13. **Load consumption of the PC at node 18 in Case 3.**

This article has been accepted for publication in a future issue of this journal, but has not been fully edited. Content may change prior to final publication. Citation information: DOI 10.1109/ACCESS.2021.3102497, IEEE Access

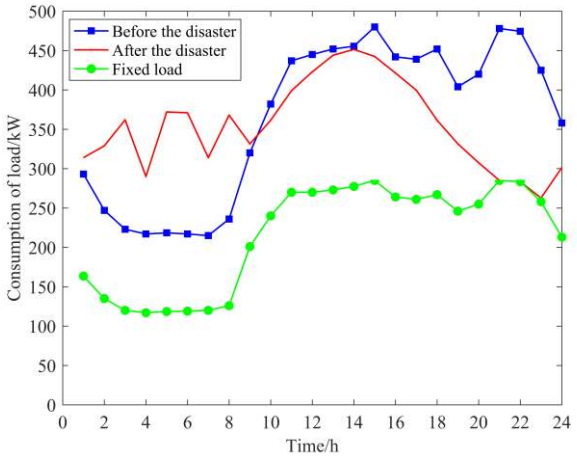

FIGURE 14. Load consumption of the PC at node 32 in Case 3.

Fig.12-14 illustrate the load consumption of three PCs before the hurricane disaster and the load consumption of three PCs after the hurricane disaster considering both multi-energy supply resources and DR resources (Case 3). Compared with Case 2, the electrical consumption pattern of nodes 14, 18, and 32 has changed in Case 3 as a result of the DR program. Partial controllable loads of each PC have shifted to the electricity valley period (from 1 am to 8 am), which reduces the peak-to-valley difference in power supply and relieves the power supply pressure during the extreme disaster event. Compared with load restoration in Case 2, the load restoration in Case 3 is further enhanced via controlling the shiftable loads (NISLs and ISLs). Therefore, implementation of the DR program contributes to further improvement of load recovery of post-disaster DS without requirements of additional equipment investment and maintenance costs. And integration of multi-energy supply-side and demand-side resources in a coordinated manner is able to maximize the restoration of the power supply of terminal loads.

VI. CONCLUSION

In this paper, we present a two-stage RO framework for determining the optimal load recovery strategy of DS with multi-energy supply-side and demand-side resources during the hurricane disaster. Comparing with the existing studies, the major contributions of this work are that we introduce a novel Z-number-based fragility modeling approach to estimate the failure probability of transmission corridors caused by extreme disasters. Besides, the effect of comprehensive utilization of power emergency resources, multi-energy supply resources, and DR resources on ELR of DS during the disaster is studied. According to the simulation results from case studies, some significant findings of this research are summarized as follows:

- Compared with the traditional fragility modeling method, the proposed Z-number-based approach can obtain a more realistic failure probability of electrical components in the power network, which considers the aging of components and credibility of fragility curves.
- Comprehensive utilization of MEGs, multi-energy coupling units, distributed generation, and DR resources are capable of maximizing the load restoration of DS during the extreme disaster, based on the complementarity of multi-energy supply-side and demand-side resources.
- Electricity customers participating in DR program conduces to the load recovery of post-disaster DS with no need for additional equipment investment and maintenance costs, which provides a more economical and flexible way to improve power grid resilience.

In this study, due to space restrictions, the multiple energy coupling of demand-side resources is not considered in the proposed resilience enhancement model. However, the interaction and substitutability of multiple energy loads can provide more potential and flexibility for the relief of pressure on energy supply during extreme disasters. Thus future works may focus on this direction for further exploring the resilience improvement resources.

REFERENCES

[1] F. Wang *et al*., "The values of market-based demand response on improving power system reliability under extreme circumstances," *Appl. Energy*, vol. 193, pp. 220-231, Feb. 2017.
[2] S. Ma, B. Chen, and Z. Wang, "Resilience enhancement strategy for distribution systems under extreme weather events," *IEEE Trans. Smart Grid*, vol. 9, no. 2, pp. 1442–1451, Mar. 2018.
[3] Y. Tan *et al*., "Distribution systems hardening against natural disasters," *IEEE Trans. Power Syst*, vol. 33, no. 6, pp. 6849–6860, Nov. 2018.
[4] S. Ma *et al*., "Resilience enhancement of distribution grids against extreme weather events," *IEEE Trans. Power Syst*., vol. 33, no. 5, pp. 4842–4853, Sep. 2018.
[5] Y. P. Fang and G. Sansavini, "Optimum post-disruption restoration under uncertainty for enhancing critical infrastructure resilience," *Reliab. Eng. Syst. Saf*., vol. 185, pp. 1–11, Dec. 2019.
[6] H. Gao, Y *et al*., "Resilience-oriented critical load restoration using microgrids in distribution systems," *IEEE Trans. Smart Grid*, vol. 7, no. 6, pp. 2837–2848, Nov. 2016.
[7] W. Yuan *et al*., "Robust optimization-based resilient distribution network planning against natural disasters," *IEEE Trans. Smart Grid*, vol. 7, no. 6, pp. 2817–2826, Nov. 2016.
[8] B. Zhang, P. Dehghanian, and M. Kezunovic, "Optimal allocation of PV generation and battery storage for enhanced resilience," *IEEE Trans. Smart Grid*, vol. 10, no. 1, pp. 535–545, Jan. 2019.
[9] K. Zou *et al*., "Distribution system restoration with renewable resources for reliability improvement under system uncertainties," *IEEE Trans. Ind. Electron*., vol. 67, no. 10, pp. 8438-8449, Oct. 2020.
[10] X. Zhang *et al*., "Restoring distribution system under renewable uncertainty using reinforcement learning," in *IEEE SmartGridComm*, Tempe, AZ, USA, Nov. 11-13, 2020.
[11] S Poudel and A Dubey, "Critical load restoration using distributed energy resources for resilient power distribution system," *IEEE Trans. Power Syst*., vol. 34, no. 1, pp. 52-63, Jan. 2019.
[12] Y. Xu *et al*., "Resilience-oriented distribution system restoration considering mobile emergency resource dispatch in transportation system," *IEEE Access*, vol. 7, pp. 73899–73912, Jun. 2019.
[13] S. Lei *et al*., "Resilient disaster recovery logistics of distribution systems: co-optimize service restoration with repair crew and mobile power source dispatch," *IEEE Trans. Smart Grid*, vol. 10, no. 6, pp. 6187–6202, Feb. 2019.
[14] A. Kavousi-Fard, M. Wang, and W. Su, "Stochastic resilient post-hurricane power system recovery based on mobile emergency resources and reconfigurable networked microgrids," *IEEE Access*, vol. 6, pp. 72311–72326, Nov. 2018.
[15] T. Ding *et al*., "A resilient microgrid formation strategy for load restoration considering master-slave distributed generators and topology reconfiguration," *Appl. Energy*, vol. 199, pp. 205–216, May. 2017.

[16] C. Chen *et al*., "Resilient distribution system by microgrids formation after natural disasters," *IEEE Trans. Smart Grid*, vol. 7, no. 2, pp. 958–966, Mar. 2015.
[17] Z. Wang *et al*., "Risk-limiting load restoration for resilience enhancement with intermittent energy resources," *IEEE Trans. Smart Grid*, vol. 10, no. 3, pp. 2507–2522, May. 2019.
[18] J. Aghaei *et al*., "Contribution of emergency demand response programs in power system reliability," *Energy*, vol. 103, pp. 688–696, May. 2016.
[19] H. G. Kwag, and J. O. Kim, "Reliability modeling of demand response considering uncertainty of customer behavior," *Appl. Energy*, vol. 122, pp. 24–33, Feb. 2014.
[20] A. Safdarian *et al*., "Distribution network reliability improvements in presence of demand response," *IET Gener. Transmiss. Distrib*., vol. 8, no. 12, pp. 2027–2035, May. 2014.
[21] P. C. Mathaios *et al*., "Power system resilience to extreme weather: fragility modeling, probabilistic impact assessment, and adaptation measures," *IEEE Trans. Power Syst*, vol. 32, no. 5, pp. 3747–3757, Sep. 2017.
[22] Y. P. Fang, and Zio E, "An adaptive robust framework for the optimization of the resilience of interdependent infrastructures under natural hazards," *Eur. J. Oper. Res*., vol. 276, pp. 1119-1136, Feb. 2019.
[23] S. Poudel, A. Dubey and A. Bose, "Risk-based probabilistic quantification of power distribution system operational resilience," *IEEE Syst. Journal*, vol. 14, no. 3, pp. 3506–3517, Sept. 2020.
[24] H. Reeves *et al*., "Prediction of land falling hurricanes with the advanced hurricane WRF model," *Mon. Weather Rev*., vol. 136, no. 6, pp. 1990–2005, Aug. 2008.
[25] G. J. Holland *et al*., "A revised model for radial profiles of hurricane winds," *Mon. Weather Rev*., vol. 138, no. 12, pp. 4393–4401, Apr. 2010.
[26] L.A. Zadeh, "A note on Z-numbers," *Inf. Sci*., vol. 181, pp. 2923–2932, Mar. 2011.
[27] B. Zeng *et al*., "Unified probabilistic energy flow analysis for electricity-gas coupled systems with integrated demand response," *IET Gener. Transmiss. Distrib*., vol. 13, no. 13, pp. 2697–2710, May. 2019.
[28] R. Flage *et al*., "Concerns, challenges, and directions of development for the issue of representing uncertainty in risk assessment," *Risk Anal*., vol. 34, no. 7, pp. 1196–1207, Jul. 2014.
[29] M. Lavorato, J. F. Franco, M. J. Rider, and R. Romero, "Imposing radiality constraints in distribution system optimization problems," *IEEE Trans. Power Syst*., vol. 27, no. 1, pp. 172–180, Feb. 2012.
[30] X. Chen, W. Wu, and B. Zhang, "Robust restoration method for active distribution networks," *IEEE Trans. Power Syst*., vol. 31, no. 5, pp. 4005–4015, Sep. 2016.
[31] S. Poudel, A. Dubey, "A two-stage service restoration method for electric power distribution systems," *arXiv preprint* arXiv:2004.07921, 2020.
[32] L. T. Marques, A. C. B. Delbem and J. B. A. London, "Service restoration with prioritization of customers and switches and determination of switching sequence," *IEEE Trans. Smart Grid*, vol. 9, no. 3, pp. 2359–2370, May. 2018.
[33] J. C. López *et al*., "Optimal Restoration/Maintenance Switching Sequence of Unbalanced Three-Phase Distribution Systems," *IEEE Trans. Smart Grid*, vol. 9, no. 6, pp. 6058–6068, Nov. 2018.
[34] S. LEI *et al*., "Routing and scheduling of mobile power sources for distribution system resilience enhancement," *IEEE Trans. Smart Grid*, vol. 10, no. 5, pp. 5650–5662, Sept. 2019.
[35] X. Zhu *et al*., "An interval-prediction based robust optimization approach for energy-hub operation scheduling considering flexible ramping products," *Energy*, vol. 194, pp. 1–16, Mar. 2020.
[36] B. Zeng *et al*., "Optimal Demand Response Resource Exploitation for Efficient Accommodation of Renewable Energy Sources in Multi-Energy Systems Considering Correlated Uncertainties," *J. Clean. Prod*., vol. 288, no. 3, pp. 125666, March. 2020.
[37] B. Zeng *et al*., "Co-optimized parking lot placement and incentive design for promoting PEV integration considering decision-dependent uncertainties," *IEEE Trans. Industr. Inform*., vol. 17, no. 3, pp. 1863-1872, March. 2021.
[38] B. Zeng *et al*., "Solving two-stage robust optimization problems using a column-and-constraint generation method," *Oper. Res. Lett*., vol. 41, pp. 457–461, Jun. 2013.
[39] IEEE PES Power System Analysis, Computing and Economics Committee, IEEE 123 Node Test Feeder, Feb. 2014. [Online]. Available: https://ewh.ieee.org/soc/pes/dsacom/testf eeders/
[40] D. Huo *et al*., "Chance-constrained optimization for multienergy hub systems in a smart city," *IEEE Trans. Ind. Electron*., vol. 66, no. 2, pp. 1402–1412, Aug. 2018.
[41] S. Bjarnadottir, Y. Li, and M. G. Stewart, "Hurricane risk assessment of power distribution poles considering impacts of a changing climate," *J. Infrastruct. Syst*., vol. 19, no. 1, pp. 12–24, Feb. 2013.

This article has been accepted for publication in a future issue of this journal, but has not been fully edited. Content may change prior to final publication. Citation information: DOI 10.1109/ACCESS.2021.3102497, IEEE Access

Xi Zhu received the B.S. and M.S. degrees in Electrical Engineering from North China Electric Power University, Beijing, China, in 2014 and 2017, and she is currently pursuing the Ph.D. degree in North China Electric Power University, Beijing, China.

Her research interests include power system operation and integrated energy system planning.

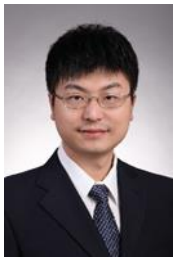

Bo Zeng (Member, IEEE) received the Ph.D. degree in electrical engineering from North China Electric Power University (NCEPU), Beijing, China, in 2014.

He is currently an Associate Professor with the Department of Electrical and Electronic Engineering of NCEPU. His current research interests include demand response modeling, electric vehicle integration, and integrated energy system planning and operation.

Yonggang Li received the Doctor degree in electrical engineering from North China Electric Power University, Baoding, Hebei, China, in 1999.

He is currently a Professor in the North China Electric Power University. His research interests include the fault diagnosis of generator.

Jiaomin Liu received the B.S. degree in automation and the Ph.D. degree from the Hebei University of Technology, Tianjin, China, in 1982 and 1998, respectively.

He is currently a Professor with the Department of Electrical and Electronic Engineering, North China Electric Power University, Baoding, China. His research interests are power system stability analysis and control including the renewable energy and power system reliability.